

Multi-wavelength Photometric and Polarimetric Observations of the Outburst of 3C 454.3 in Dec. 2009

Mahito SASADA¹, Makoto UEMURA², Yasushi FUKAZAWA¹, Koji S. KAWABATA², Ryosuke ITOH¹, Itsuki SAKON³, Kenta FUJISAWA^{4,5}, Akiko KADOTA⁴, Takashi OHSUGI², Michitoshi YOSHIDA², Hajimu YASUDA¹, Masayuki YAMANAKA¹, Shuji SATO⁶, and Masaru KINO⁶

¹*Department of Physical Science, Hiroshima University, Kagamiyama 1-3-1, Higashi-Hiroshima 739-8526
sasada@hep01.hepl.hiroshima-u.ac.jp*

²*Astrophysical Science Center, Hiroshima University, Kagamiyama 1-3-1, Higashi-Hiroshima 739-8526*

³*Department of Astronomy, Graduate School of Science, the University of Tokyo, 7-3-1 Hongo, Bunkyo-ku, Tokyo 113-0033*

⁴*Graduate school of Science and Engineering, Yamaguchi University, 1677-1 Yoshida, Yamaguchi, Yamaguchi 753-8512*

⁵*The Research Institute for Time Studies, Yamaguchi University, 1677-1 Yoshida, Yamaguchi, Yamaguchi 753-8511*

⁶*Department of Physics, Nagoya University, Furo-cho, Chikusa-ku, Nagoya 464-8602*

(Received 2011 April 18; accepted 2011 December 15)

Abstract

In December 2009, the bright blazar, 3C 454.3 exhibited a strong outburst in the optical, X-ray and gamma-ray regions. We performed photometric and polarimetric monitoring of this outburst in the optical and near-infrared bands with TRISPEC and HOWPol attached to the Kanata telescope. We also observed this outburst in the infrared band with *AKARI*, and the radio band with the 32-m radio telescope of Yamaguchi University. The object was in an active state from JD 2455055 to 2455159. It was 1.3 mag brighter than its quiescent state before JD 2455055 in the optical band. After the end of the active state in JD 2455159, a prominent outburst was observed in all wavelengths. The outburst continued for two months. Our optical and near-infrared polarimetric observations revealed that the position angle of the polarization (PA) apparently rotated clockwise by 240 degrees within 11 d in the active state (JD 2455063—2455074), and after this rotation, PA remained almost constant during our monitoring. In the outburst state, PA smoothly rotated counterclockwise by 350 degrees within 35 d (JD 2455157—2455192). Thus, we detected two distinct rotation events of polarization vector in opposite directions. We discuss these two events compared with the past rotation events observed in 2005, 2007 and 2008.

Key words: BL Lacertae Objects: individual: 3C 454.3 — polarization — infrared: general

1. Introduction

Blazar is a class of active galactic nuclei, whose relativistic jets are considered to be directed along the line of sight (e.g. Blandford et al. 1979). Radiation of blazars has three main properties. First, the blazars emit electromagnetic radiation in a broad range from the radio to gamma-ray bands. Their emission consists of two major components (e.g. Kubo et al. 1998). The low energy component is synchrotron radiation observed from the radio to the optical, sometimes extending to the X-ray bands. The high energy component is inverse-Compton scattering from the X-ray to the gamma-ray bands. Second, blazars exhibit rapid and violent variability in all wavelength bands (Antonucci 1993). The variability has various timescales from less than a day (e.g. Aharonian et al. 2007; Albert et al. 2007; Sasada et al. 2008; Raiteri et al. 2008b) to longer than years (e.g. Sillanpää et al. 1996). Third, blazars possess relativistic jets (e.g. Lister et al. 2009), which are responsible for high polarization observed at optical/near-infrared (NIR), and radio wavelengths. Since the polarization can be a probe of the magnetic field in the jet, polarimetric observations are important to study the structure of the jet.

The temporal variation of the polarization vector is complex in general. Jones et al. (1985) reported that the polarization behavior was erratic in blazars. On the other hand, several papers reported that the polarization vector exhibited systematic variations, for example, positive correlations between the flux and the degree of polarization (PD) (e.g. Smith et al. 1986). Recently, Marscher et al. (2008) have reported that the polarization vector in BL Lac smoothly rotated when the object was bright. From this result, they proposed that this rotation indicated an emission zone passing through a helical magnetic field in the jet. Abdo et al. (2010a) reported a rotation of polarization in 3C 279, and proposed that the rotation event is attributed to a bent jet. However, there are only a few rotation events which have been reported to date.

3C 454.3 is one of the most famous blazars. The object is classified as Flat Spectrum Radio Quasars (FSRQs), and its redshift is $z = 0.859$ (Jackson & Browne 1991). Although the object had been quiet in the optical band until 2001, the object has kept showing the active behavior since then (Villata et al. 2006). In 2005, the object showed an exceptional outburst. In this outburst, the object brightened from the radio to the gamma-ray bands (Fuhrmann et al. 2006; Pian et al. 2006; Giommi et al.

2006 ; Villata et al. 2007). After this outburst, similar outbursts were detected in 2007 and 2008. In 2005 and 2007 outbursts, rotation events of the optical polarization vector were reported by Jorstad et al. (2010) and Sasada et al. (2010). In Dec. 2009, a prominent outburst was reported for this object in the gamma-ray band by *Fermi*/LAT and AGILE (Striani et al. 2009a; Striani et al. 2009b; Escande & Tanaka 2009; Striani et al. 2010; Pacciani et al. 2010; Ackermann et al. 2010), in the X-ray band by *INTEGRAL*/IBIS (Vercellone et al. 2009), by *Swift*/XRT (Sakamoto et al. 2009), by *Swift*/BAT (Krimm et al. 2009), in the optical bands (Villata et al. 2009a; Bonning et al. 2009; Sasada et al. 2009). The object was the brightest source in the GeV-gamma-ray sky for over a week (Ackermann et al. 2010). The object showed flux variability over timescales less than three hours and very mild spectral variability with an indication of gradual hardening preceding major flares. The minimum Doppler factor was 13, estimated by using these results. Bonnoli et al. (2011) also estimated the Doppler factors ~ 25 during the outburst by constructing a multi-wavelength spectral model.

We performed monitor observations of 3C 454.3 from May 2009 to February 2010 in a multi-color photometric and polarimetric mode using the Kanata telescope. We also observed in the radio and infrared (IR) bands. In this paper, we report on the behavior of the 2009 outburst in these bands, and the detections of two rotation events in the polarization vector. Directions of these two rotations were different, suggesting a complex magnetic field in the jet. This paper is arranged as follows: In section 2, we present the observation method and analysis in the radio, infrared, optical and X-ray bands. In section 3, first we report the light curves and the spectral indexes of the X-ray and optical bands. Then, we report the temporal behavior of polarization in the optical and NIR bands. After that, we report the spectral energy distribution from the radio to optical band. In section 4, we discuss two rotation events which we detected, by comparing them with the past rotation events observed in 2005, 2007 and 2008. The conclusion is drawn in section 5.

2. Observation

2.1. TRISPEC and HOWPol attached to the Kanata telescope

We performed monitor observations of 3C 454.3 using TRISPEC attached to the Cassegrain focus of the Kanata 1.5-m telescope at Higashi-Hiroshima Observatory. TRISPEC can perform photometric and polarimetric observations in the optical and two NIR bands, simultaneously (Watanabe et al. 2005). In the observation of 3C 454.3, unfortunately, one of the two NIR arrays was not available due to a readout error. Therefore, we observed the object with the multi-color photometric and polarimetric monitoring in the V and J bands. A unit of the observing sequence consisted of successive exposures at four position angles of a half-wave plate; 0° , 45° , 22.5° , 67.5° . A set of polarization parameters was derived from

each set of the four exposures.

We also observed in the multi-color photometric mode in the R_C and I_C bands during the outburst of the object using HOWPol (Hiroshima One-shot Wide-field Polarimeter; Kawabata et al. 2008) attached to a Nasmyth focus of the Kanata telescope. In this paper, we use multi-band photometric data obtained with HOWPol in § 3.3.

The integration time depended on the sky condition and the brightness of 3C 454.3. Typical integration times were 90 and 85 s in the V and J bands, respectively. All images were bias-subtracted and flat-fielded, before aperture photometry. We performed differential photometry with a comparison star taken in the same frame of 3C 454.3. Its position is R.A.= $22^{\text{h}}53^{\text{m}}58^{\text{s}}.11$, Dec.= $+16^\circ09'07''.0$ (J2000.0) and its magnitude is $V=13.587$, $R_C=13.035$, $I_C=12.545$ and $J=11.858$ (González – Pérez et al. 2001; Skrutskie et al. 2006). After the differential photometry, we calculated the flux, assuming that the 0 mag corresponds to the flux with 1.98, 1.42, 0.895 and 0.384×10^{-5} erg cm $^{-2}$ s $^{-1}$ in the V , R_C , I_C and J bands (Fukugita Simasaku & Ichikawa 1995; Bessell, Castelli & Plez 1998).

We confirmed that the instrumental polarization was smaller than 0.1 % in the V and J bands using the observation of unpolarized standard stars. We, hence, applied no correction for it. The instrumental depolarization factors, $\alpha_{V\text{dep}}$ and $\alpha_{J\text{dep}}$, was derived from the observation using Glan-Taylor prism, to be $\alpha_{V\text{dep}}=0.827$ and $\alpha_{J\text{dep}}=0.928$. The observation was corrected for it. The zero point of the position angle of polarization (PA) is defined by the standard system (measured from north to east) by observing the polarized stars, HD 19820 and HD 25443 (Wolff, Nordsieck & Nook 1996).

2.2. Swift/XRT

We utilized the archival data of Swift/XRT for deriving the X-ray light curve. The XRT observations were carried out using the Photon Counting (PC) readout mode. The XRT data were reduced using FTOOLS in the HEASoft package (v6.6). We extracted the source event within a radius of $50''$ and background event within radii of 80 – $100''$ centered on the source. We used the XSPEC package (v11.3) to fit the data. We applied an absorbed power-law model with Galactic absorption fixed at a value of $N_H = 1.1 \times 10^{21}$ cm $^{-2}$ (wabs*powerlaw model in XSPEC) (Donnarumma et al. 2009).

2.3. AKARI

The NIR spectroscopic observations of 3C 454.3 were carried out at 14:42:27 on 12 Dec., 15:25:22 on 13 Dec. and 01:18:31 on 14 Dec. in 2009(UT) with the AKARI satellite in the framework of the AKARI Open Time Observing programs for the Phase 3-II “Blazar Variability in near-Infrared, Optical and Gamma-ray regions (BVIOG)” (PI: M. Sasada). All the observations were performed with the spectroscopic mode (AOT IRCZ4; Onaka et al. 2010) in which the data were taken with the prism, NP (1.8–5.5 μm ; Ohyama et al. 2007), installed in the NIR channel of the Infrared Camera (IRC; Onaka et al. 2007) of the AKARI satellite. Each of the data reduction proce-

cedure, including the subtraction of the detector dark current, correction for the high-energy ionizing particles effects, the shift and co-addition of the exposure frames, and the wavelength calibration for NP data, follows those in the IRC Spectroscopy toolkit for Phase 3 data Version 20110114. In order to correct for the sensitivity changes during the phase-3 of *AKARI* mission to obtain the accurate flux level of the spectrum due to the seasonal temperature fluctuations of the detectors, we derived our own system spectral response curve of NP by using the spectroscopic datasets of a calibration standard KF06T2 collected at the nearest epochs of our datasets. In this paper, we used only 3.0–5.0 μm data because of a large uncertainty of the flux calibration outside this region.

2.4. Yamaguchi radio telescope

The radio observation was carried out with the Yamaguchi 32-m radio telescope at the center frequency of 8.38 GHz and bandwidth of 400 MHz in the total power mode. The antenna temperatures were measured at the position of 3C 454.3 and at four positions 2 arc-min (a half of FWHM) offset to positive and negative in both azimuth and the elevation directions from the target so as to obtain the true antenna temperature by correcting the pointing error of the telescope. A flux calibrator 3C 48 was observed at the same elevation of 3C 454.3. The flux density of 3C 454.3 was determined from the ratio of the antenna temperatures of 3C 454.3 to 3C 48, and the flux density of 3C 48 (3.34 Jy, Ott et al. 1994). The accuracy of the measured flux density is supported to be 5 % empirically. The observation was ensured to be 5 times from October 21st to December 7th.

3. Result

3.1. Photometry

Figure 1 shows the light curves in the X-ray and optical bands, temporal variation of photon index Γ and the $V - J$ color variation. The X-ray and optical light curves show that the flux of 3C 454.3 was variable, and we define three states based on the light-curve structure. The first state is a quiescent state from the start date of our monitoring to JD 2455055. The second state is an active state from JD 2455055 to 2455159. And the third state is an outburst state after JD 2455159. The flux in the quiescent state was less variable and faint both in the X-ray and optical bands compared with the flux after the active state. The active state was characterized by several short and small flares with duration of ~ 10 d and amplitude of a factor $\lesssim 3$. On JD 2455159, the object had suddenly become bright both in the X-ray and optical band, simultaneously. In the decline phase of the outburst, we can estimate a decline rate, τ , assuming that the flux follows an exponential decay, that is, $F(t) \propto e^{-t/\tau}$ (Böttcher et al. 2007). The decline rates were 14 ± 2 and 49 ± 3 d in the X-ray and optical bands. Hence, the flux decline in the X-ray band was faster than that in the optical band.

Radio observations at 8.38 GHz were also performed in JD 2455125, 2455127, 2455133 and 2455172 by Yamaguchi

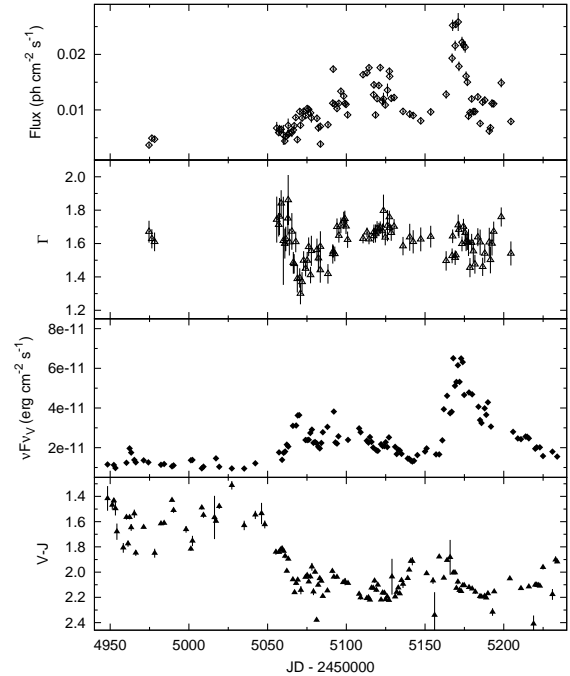


Fig. 1. Light curves, temporal variation of photon index and color variation of 3C 454.3. From top to bottom, the panels show the light curve and temporal variation of photon index Γ in the X-ray band at 1 keV, the light curve in the V band and $V - J$ color variation.

radio observatory as mentioned in § 2.4. The radio flux density was constant at 8.1 Jy and no significant change was observed during the active and outburst states. The lack of a tight correlation between the radio and optical fluxes was also reported in past studies of 3C 454.3 (Villata et al. 2007).

The photon index in the X-ray band, Γ was almost constant during our monitoring period, except for a possible variations at the onset of the active state; a temporary softening of spectra can be seen in \sim JD 2455070, while its variation amplitude is small. Raiteri et al. (2011) also analyzed the same XRT data, and reported that no real changes in Γ could be detected from 2008 to 2010. It is also noteworthy that no prominent change in Γ was associated with the outburst state.

In the quiescent state, $V - J$ was about 1.6. The $V - J$ color in the quiescent state was bluer than those in the active and outburst states. This feature indicates a, so-called, redder-when-brighter trend. The same color behavior was reported in past observations of 3C 454.3 (e.g. Raiteri et al. 2008a; Sasada et al. 2010). It is widely accepted that this feature appears because an underlying thermal emission in the UV band, called as Big Blue Bump; BBB, is bluer than the variable synchrotron emission (Raiteri et al. 2007).

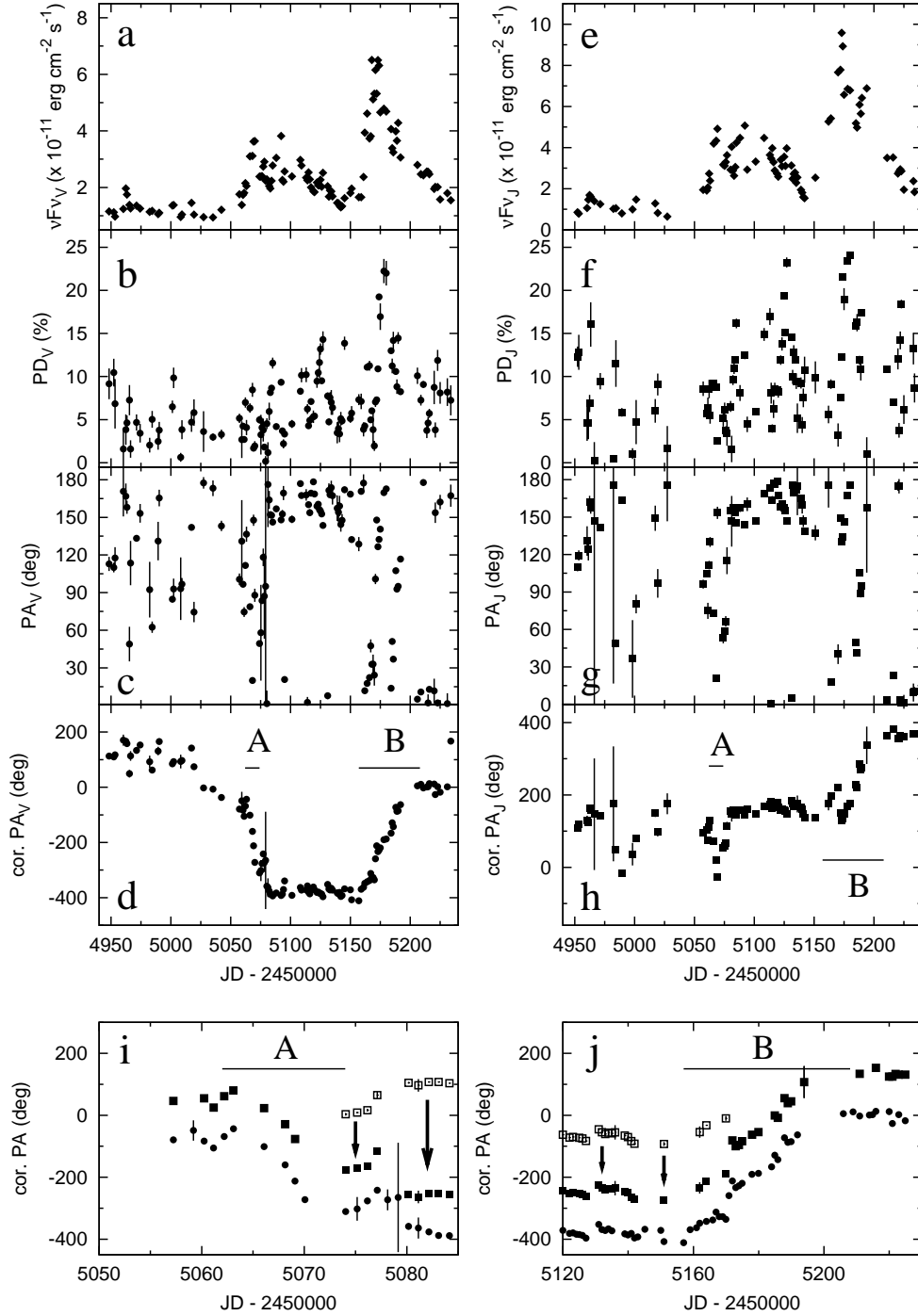


Fig. 2. Temporal variations of the flux and polarization parameters. The left and right panels from “a” to “h” show the each variation in the V and J bands. The top panels show the light curves of the object. The second, third and fourth panels show the temporal variations of the PD and PA and the corrected PA. The bottom panels show temporal variations of the corrected PA focused on the rotation “A” and “B”. The filled circle shows the polarization parameters in the V band, and the open and filled squares show the polarization parameters in the J band.

3.2. Polarimetry

Figure 2 shows the light curves and temporal variations of the polarization parameters in the V and J bands. The panel “b”, “c”, “f” and “g” show the temporal variation of the PD and PA in the V and J bands. The PD in the active and outburst states exhibited large variations compared with the PD in the quiescent state. The averaged PD_V were 4.5, 6.0 and 8.9 % and the averaged PD_J were 7.3, 9.2 and 12.2 % in the quiescent, active and outburst states, respectively. In the outburst state, the maxima of the PD_V and PD_J were 22.0 ± 1.4 and 24.1 ± 0.4 % on JD 2455180. The averaged PD_J were higher than the averaged PD_V in all states. The high PD in the J band is partly due to a low contribution of the unpolarized flux from the BBB component in the J band.

We corrected the PA assuming that the temporal variation in the PA is less than 90° between neighbor two observations. We defined the variation as $\Delta PA_n = PA_{n+1} - PA_n - \sqrt{\delta PA_{n+1}^2 + \delta PA_n^2}$, where PA_{n+1} and PA_n were the $n+1$ - and n -th PA and δPA_{n+1} and δPA_n were the errors of $n+1$ - and n -th PA. If $\Delta PA_n < -90^\circ$ ($> +90^\circ$), we add $+180^\circ$ (-180°) to PA_{n+1} . If $|\Delta PA_n| < 90^\circ$, we performed no correction of PA_{n+1} . The panel “d” and “h” show the corrected PA.

In the panel “d”, two rotation events can be seen, “A” and “B”. The rotation event “A” occurred from JD 2455063 to 2455074 when the object entered the active state. The rotation event “B” occurred from JD 2455157 to 2455192, during the outburst state. In the quiescent state, there was no rotation event. Thus, we can consider that these rotation events were associated with the activity of the object. After the rotation “A”, the PA was constant during the active state, at about $170^\circ \pm 30^\circ$.

These rotations can be confirmed also in the J -band observations, while the timings of the PA correction are different in several points as shown in panel “h”. This is mostly due to large errors of PA (δPA) in the J -band observations. The PA correction mentioned above depends on δPA . In addition, the data number of the J -band observation is smaller than that of the V -band one. This is partly due to mechanical errors of our NIR detector. Thus, the PA correction for the V -band data is more reliable than that for the J -band one. For example, in panels “i” and “j”, we show the corrected PA around rotations “A” and “B”. The open squares denote the corrected PA of the J -band data. They apparently show different behavior from the V -band PA (the filled circles). However, they become consistent if -180 or -360 deg is added to the J -band PA. It demonstrates that the V - and J -band data have the same behavior if the ± 180 deg ambiguity in PA is taken into account.

Rotation rates of “A” and “B” were estimated as -26 ± 2.3 and $+9.8 \pm 0.5$ deg d^{-1} , calculated by a linear regression model of PA. If the rotation rate is positive, the rotation direction is counterclockwise in the QU plane, or the celestial sphere, and vice versa. Figure 3 shows the temporal variation of the object in the Stokes QU plane in the V band. The direction of “A” was clockwise and

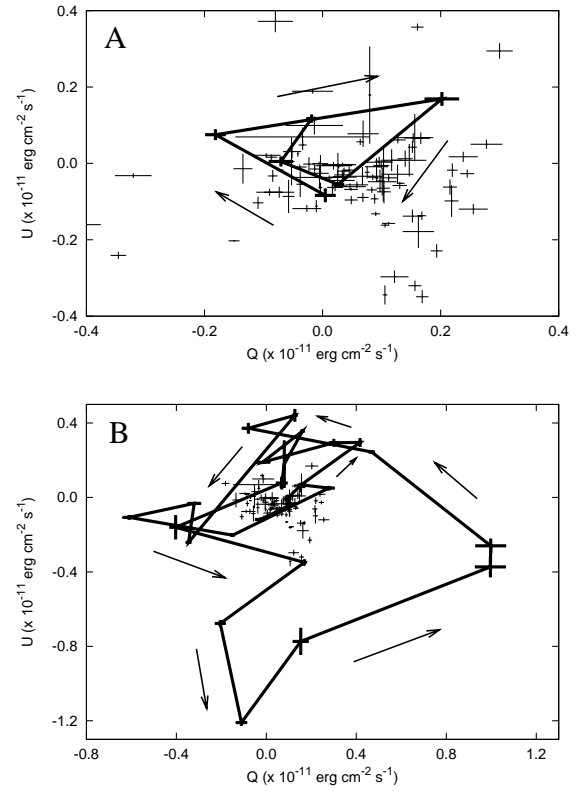


Fig. 3. Behavior of the polarization Stokes parameters on the QU planes during the rotation “A” and “B” in the V band.

that of “B” was counterclockwise in the QU plane, as can be seen in the top and bottom panels of figure 3. Thus, the directions of these two rotations were different.

Figure 4 shows the light curve and temporal variations of polarization parameters during the outburst state in the V band. The solid line was the best-fitted linear function for the corrected PA from JD 2455157 to 2455192. In the fourth panel, we show the residual PA from the linear function. The PD was low during the early phase of the outburst. After the outburst maximum, it became high. The residual PA was largely deviated from zero around JD 2455170 (the forth panel of figure 4). Around this deviation epoch, the V band magnitude was at the maximum (the top panel of figure 4) and the PD_V was minimum (~ 2 %; the second panel of figure 4).

3.3. Spectrum in the NIR band and spectral energy distribution

We also obtained the NIR spectroscopic data with *AKARI*/IRC during the outburst state. In the top panel of figure 4, the arrows represent the observation epochs with *AKARI*. The NIR fluxes and the shape of the spectra were almost identical within the $1-\sigma$ error level among the three observation epochs. The bottom panel of figure 4 shows the averaged spectrum of 3C 454.3. The spectrum is dominated by featureless red continuum emission, in-

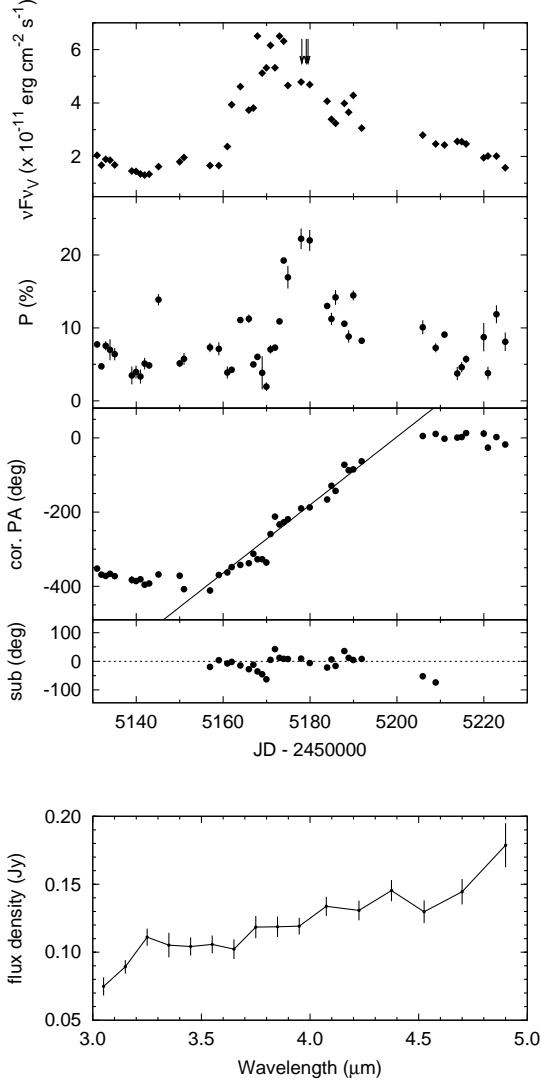


Fig. 4. Temporal variation of the flux, polarization parameters, the PA subtracted from the linear function fitted the data from JD 2455157 to 2455192 in the V band and spectrum in the NIR region. The arrows in the top panel are the epochs of the *AKARI* observations. The bottom panel shows the averaged spectrum of three spectra.

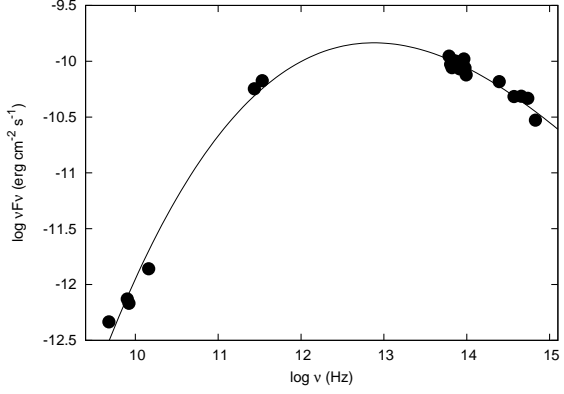


Fig. 5. Spectral energy distribution from the radio to optical bands during the outburst state. The solid line represents the best fitted third-order log-polynomial function.

indicating that the synchrotron radiation was dominant in this wavelength range during the outburst state.

We show the spectral energy distribution (SED) of the object from the radio to optical regions during the outburst state in figure 5. The NIR data points are the average flux for three epochs obtained with *AKARI*. As for the optical data, the figure includes the observation with Kanata which was obtained on JD 2455180, closest to the *AKARI* observations. In the radio band, we use public data observed with the Submillimeter Array (SMA; 1 mm on JD 2455181 and $850 \mu\text{m}$ on JD 2455176), the the University of Michigan Radio Astronomy Observatory (UMRAO; 4.8 on JD 2455169.5, 8.0 on JD 2455184.5 and 14.5 GHz on JD 2455179.5) and our data observed with the Yamaguchi radio telescope (8.38 GHz on JD 2455172). All radio data are obtained within 10 d of our *AKARI* observations. The SMA data was obtained as part of the SMA flux density monitoring program and used by permission (Gurwell et al. 2007). The optical and NIR data were corrected for the Galactic interstellar extinction based on Schlegel et al. (1998). The extinction for the *AKARI* data were estimated by interpolating the extinctions from 3 to $5 \mu\text{m}$ obtained from Schlegel et al. (1998). The solid line represents the best fitted third-order log-polynomial function. The peak frequency of the synchrotron component was estimated as $7.6 \times 10^{12} \text{ Hz}$. This is the same order of magnitude as the values reported in previous studies (e.g. Raiteri et al. 2008b; Abdo et al. 2010b). The optical and NIR data are smoothly connected, which suggests that at least the emission from the NIR to optical energy band can be explained by a synchrotron component.

4. Discussion

4.1. Implication of polarimetric behavior during an outburst state in 2009

Our monitoring observations suggest that two rotation events of polarization occurred during the active and outburst states of 3C 454.3 in 2009. The features of the

rotation “A” and “B” were summarized in table 1. The rotation rates, directions and periods of the rotations are different between the rotation “A” and “B”.

Two models have recently been proposed for the rotation of polarization; Marscher et al. (2008) and Abdo et al. (2010a). According to Marscher et al. (2008), a rotation of the polarization vector is a sign of helical magnetic field in the jet. The directions of the rotation events in 3C 454.3 are both clockwise and counterclockwise. In the case of the simple helical magnetic field in the jet, the direction of the rotation of polarization should be one-side. Thus, it needs more complex magnetic field structure in order to explain the rotation events in 3C 454.3.

Abdo et al. (2010a) reported a rotation event in 3C 279, and suggested a non-axisymmetric structure of the jet, implying a curved trajectory for the emitting material. This idea can explain rotations in both directions, and hence, the rotations in 3C 454.3. We can estimate the distance, Δr , traveled by the emitting material during the well-sampled rotation “B” in 2009. We calculate the travel distance Δr as $\Gamma_{\text{jet}}^2 c \Delta t$, where Γ_{jet} is the bulk Lorentz factor, c is the speed of light and Δt is the duration of the rotation event (Abdo et al. 2010a). The duration of the rotation “B” was 35 d. In this case, we adopt a values of $\Gamma_{\text{jet}} = 19.6$ which was reported by Bonnoli et al. (2011) with the data on JD 2455167.5 (2 Dec. 2009). Thus, we calculate $\Delta r \approx 3.5 \times 10^{19}$ cm. The travel distance of our result was the same order of magnitude compared with that for 3C 279 reported in Abdo et al. (2010a). On the other hand, the duration of the rotation “A” was shorter than that of the rotation “B”. Thus, the travel distance of the rotation “A” could be shorter than that of “B” if Γ_{jet} in the active state is same or smaller than that in the outburst state.

Sasada et al. (2011) reported that there was a positive correlation between the amplitudes of the flux and PD of flares in 41 blazars. The large-amplitude variations in the flux and PD were shown in the outburst state. Thus, there was a positive correlation between the amplitudes of the flux and PD in the outburst state of 3C 454.3, which was consistent with the positive correlation in blazar flares found by Sasada et al. (2011).

The peak of the PD was delayed by 10 d from the peak of the flux in the outburst. This behavior might be explained by the following simple geometrical effect scenario. Laing (1980) suggest that the PD is the highest when the line-of-sight is parallel to the shock plane in the co-moving frame. In this assumption, the observed flux from the jet is low because of a low Doppler factor. When the line-of-sight is perpendicular to the shock plane, the observed flux is high because of a high Doppler factor, and PD is low because the magnetic field direction is not aligned. Hence, in this scheme, if the shock comes toward us just after its formation then the shock plane gradually inclines with respect to line-of-sight, the PD rises up after the flux peak. It should be noted that the Doppler factor is changed in this scenario. The Doppler factor during the 2009 outburst was estimated with multi-wavelength spectral models, which indicate that the Doppler factor δ was almost

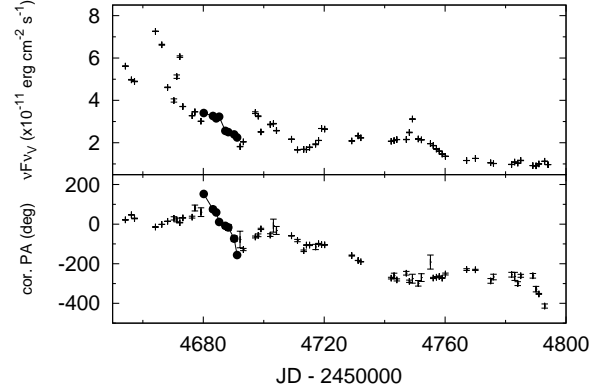


Fig. 6. Temporal variations of the corrected PA in 2008. The top panel shows the light curve in the V band. The bottom panel shows the temporal variation of the corrected PA in the same band. Filled circles show the rotation event in 2008.

constant, $\delta \sim 25 - 28.5$ during the outburst (Ackermann et al. 2010; Bonnoli et al. 2011). The observed flux, $F_{\nu, \text{obs}}$, from the shocked region depends strongly on δ , as $F_{\nu, \text{obs}} \propto \delta^{3+\alpha}$, where α is a spectral index. During the period of rotation “B” (JD 2455157–2455192), the maximum and minimum V-band flux were 6.501 and 1.658 $\times 10^{-11}$ erg cm $^{-2}$ s $^{-1}$, indicating the flux changed by a factor of 3.9. However, the amplitude of the flux variation should be larger than that, because the J-band flux variation was larger than that in the V band. If we explain all the flux variation only by the variation in δ , δ should be changed at least by a factor of 1.4, assuming the spectral index, $\alpha = 1$. This is, however, apparently inconsistent with the result from SED modeling that it was constant within $\delta \sim 24.5 - 28.5$. Thus, it would be difficult to explain the observation only by the variation in δ . More detailed and complex jet modeling would be needed for interpreting the behaviors of the flux and polarization in the outburst state.

4.2. Comparison in five rotation events

Other rotation events were also reported in active states of 3C 454.3 in 2005 and 2007. Jorstad et al. (2010) reported that the optical outbursts in 2005 autumn and in 2007 were accompanied by systematic rotation of the PA. Sasada et al. (2010) also reported a rotation event in the 2007 outburst.

In 2008, 3C 454.3 had an outburst in the radio, optical, X-ray and gamma-ray bands (Abdo et al. 2009 ; Villata et al. 2009b). We also monitored the object during the 2008 outburst with Kanata/TRISPEC in multi-color photometric and polarimetric mode. Figure 6 shows the light curve and temporal variation of the corrected PA in the V band in 2008 and 2009. The object reached its outburst maximum on \sim JD 2454664. The object stayed active even after the maximum, until \sim JD 2454760, and then it returned to quiescence. In the lower panel of figure 6, we can see a gradual decreasing trend of the PA just after the outburst maximum, which apparently continued until

Table 1. Rotation rates in each rotation event.

Event	Rate (deg d ⁻¹)	Total (deg)	rotation period JD–2450000
2005	8.7 ± 1.1	—	—
2007	22.0 ± 3.0	130	4333—4338
2008	−27.0 ± 2.0	300	4680—4691
2009 “A”	−26.0 ± 2.3	270	5063—5074
2009 “B”	9.8 ± 0.5	350	5157—5192

The 2005 and 2007 rotation events were reported by Jorstad et al. (2010) and Sasada et al. (2010).

the object returned to quiescence. In addition, there is a sign of a rapid and short rotation of polarization between JD 2454680 and 2454691, as indicated with the filled circle in figure 6.

To date, five rotation events of polarization were reported in 3C 454.3 during its active and outburst states in 2005, 2007, 2008 and 2009. We summarize their rotation rates, total degree of the rotation in table 1. We also show the periods of the rotation events, which we used for estimating the rotation rates. Three rotation rates are positive values and two rates are negative. Thus, there are not only counterclockwise, but also clockwise directions of the PA rotations. Another feature of the rotation events is that there seems to be two types of events; fast rotation events (2007, 2008 and 2009 “A”) and slow rotation events (2005 and 2009 “B”). The fast ones have the absolute rate of the rotation larger than 20 deg d⁻¹, whereas the slow ones have the value smaller than 10 deg d⁻¹. Time durations of two types of rotations are different. The fast ones have short durations, less than 11 d, and the slow rotation “B” in 2009 has a long duration, 35 d. It could partly be an observational bias because it is difficult to detect short and slow rotation events. However, it is worth nothing that there was not any long and fast rotation from 2007 to 2009.

One possibility is that the fast rotation is the result of an erratic behavior of the polarization vector. Villforth et al. (2010) reported that the polarization vector can be separated into two components: an optical polarization core and chaotic jet emission. If the chaotic polarization component with a short timescale moves around the origin of the *QU* plane, a short fast rotation can occur. Ikejiri et al. (2011) also discussed that a rotation episode indicated only by a few data points cannot be distinguished from results of a random walk in the *QU* plane.

5. Conclusion

We performed the photometric and polarimetric monitoring of 3C 454.3 during 2009–2010. The object showed the active and outburst states in the optical and near-infrared light curves and two rotation events in the temporal variations of polarization. In the past and our polarimetric monitoring, five rotation events were reported in 3C 454.3. The rotations were observed in both clockwise and counterclockwise directions in

the *QU* plane. The complex model of the structure of the magnetic field in the jet is needed to explain these rotation events.

This work was partly supported by a Grand-in-Aid from the Ministry of Education, Culture, Sports, Science, and Technology of Japan (22540252.). This research has made use of data from the University of Michigan Radio Astronomy Observatory which has been supported by the University of Michigan and by a series of grants from the National Science Foundation, most recently AST-0607523. The Submillimeter Array is a joint project between the Smithsonian Astrophysical Observatory and the Academia Sinica Institute of Astronomy and Astrophysics and is funded by the Smithsonian Institution and the Academia Sinica. M. Sasada and M. Yamanaka have been supported by the JSPS Research Fellowship for Young Scientists.

References

- Abdo, A. A. et al. 2009, *ApJ*, 699, 817
- Abdo, A. A. et al. 2010a, *Nature*, 463, 919
- Abdo, A. A. et al. 2010b, *ApJ*, 716, 30
- Ackermann, M., et al. 2010, *ApJ*, 721, 1383
- Aharonian, F., et al. 2007, *ApJ*, 664, L71
- Albert, J., et al. 2007, *ApJ*, 669, 862
- Antonucci, R. 1993, *ARA&A*, 31, 473
- Bessell, M. S., Castelli, F., & Plez, B. 1998, *A&A*, 333, 231
- Blandford, R. D., & Königl, A. 1979, *ApJ*, 232, 34
- Bonning, E., et al. 2009, *ATel*, 2332, 1
- Bonnoli, G., Ghisellini, G., Foschini, L., Tavecchio, F., & Ghirlanda, G. 2011, *MNRAS*, 410, 368
- Böttcher, M., et al. 2007, *ApJ*, 670, 968
- Donnarumma, I., et al. 2009, *ApJ*, 707, 1115
- Escande, L., & Tanaka, Y. T. 2009, *ATel*, 2328, 1
- Fuhrmann, L., et al. 2006, *A&A*, 445, L1
- Fukugita, M., Shimasaku, K., & Ichikawa, T. 1995, *PASP*, 107, 945
- Giommi, P., et al. 2006, *A&A*, 456, 911
- González – Pérez, J.N., Kidger, M.R., & Martín – Luis, F. 2001, *AJ*, 122, 2055
- Gurwell, M. A., Peck, A. B., Hostler, S. R., Darrah, M. R., & Katz, C. A. 2007, in *ASP Conf. Ser. 375, From Z-Machines to ALMA: (Sub)Millimeter Spectroscopy of Galaxies*, ed. A. J. Baker et al. (San Francisco, CA: ASP), 234
- Ikejiri, Y., et al. 2011, *PASJ*, 63, 639
- Jackson, N., & Browne, W. A. 1991, *MNRAS*, 250, 414
- Jones, T. W., Rudnick, L., Fiedler, R. L., Aller, H. D., Aller, M. F., & Hodge, P. E. 1985, *ApJ*, 290, 627
- Jorstad, S.G., et al. 2010, *ApJ*, 715, 362
- Kawabata, K. S., et al. 2008, in *Society of Photo-Optical Instrumentation Engineers (SPIE) Conference Series*, Vol. 7014, Society of Photo-Optical Instrumentation Engineers (SPIE) Conference Serie
- Krimm, H. A., et al. 2009, *ATel*, 2330, 1
- Kubo, H., Takahashi, T., Madejski, G., Tashiro, M., Makino, F., Inoue, S. & Takahara, F. 1998, *ApJ*, 504, 693
- Laing, R. A. 1980, *MNRAS*, 193, 439
- Lister, M. L., Homan, D. C., Kadler, M., Kellermann, K. I., Kovalev, Y. Y., Ros, E., Savolainen, T., Zensus, J. A. 2009, *ApJ*, 696, L22

- Marscher, A.P., et al.2008, *Nature*, 452, 966
Ohyama, Y., et al.2007, *PASJ*, 59, 411
Onaka, T., et al.2007, *PASJ*, 59, 401
Onaka, T., et al.2007, *Proc. of SPIE*, 7731, 16
Ott, M., Witzel, A., Quirrenbach, A., Krichbaum, T. P.,
Standke, K. J., Schalinski, C. J., & Hummel, C. A. 1994,
A&A, 284, 331
Pacciani, L., et al.2010, *ApJ*, 716, L170
Pian, E., et al.2006, *A&A*, 449, 21
Raiteri C. M., et al.2007, *A&A*, 473, 819
Raiteri C. M., et al.2008, *A&A*, 485, L17
Raiteri C. M., et al.2008, *A&A*, 491, 755
Raiteri C. M., et al.2011, *A&A*, 534, 87
Sasada, M., et al.2008, *PASJ*, 60, L37
Sasada, M., et al.2009, *ATel*, 2333, 1
Sasada, M., et al.2010, *PASJ*, 62, 645
Sasada, M., et al.2011, *PASJ*, 63, 489
Sakamoto, T., D'Ammando, F., Gehrels, N., Kovalev, Y. Y.,
& Sokolovsky, K. 2009, *ATel*, 2329, 1
Schlegel, D. J., Finkbeiner, D. P., & Davis, M. 1998, *ApJ*, 500,
525
Sillanpää, A., et al.1996, *A&A*, 305, L17
Skrutskie, M. F., et al.2006, *AJ*, 131, 1163
Smith, P. S., Balonek, T. J., Heckert, P. A., & Elston, R. 1986,
ApJ, 305, 484
Striani, E., et al.2009a, *ATel*, 2322, 1
Striani, E., et al.2009b, *ATel*, 2326, 1
Striani, E., et al.2010, *ApJ*, 718, 455
Vercellone, S., et al. 2009, *ATel*, 2344, 1
Villata, M., et al.2006, *A&A*, 453, 817
Villata, M., et al.2007, *A&A*, 464, L5
Villata, M., Raiteri, C. M., Larionov, V. M., Konstantinova, T.
S., Nilsson, K., Pasanen, M., & Carosati, D. 2009a, *ATel*,
2325, 1
Villata, M., et al.2009b, *A&A*, 504, L9
Villforth, C., et al.2010, *MNRAS*, 402, 2087
Watanabe, M., et al.2005, *PASP*, 117, 870
Wolff, M. J., Nordsieck, K. H. & Nook, M. A. 1996, *AJ*, 111,
856